Theoretical Study on the *Tropos* Nature of the BIPHEP−Pd(II)/DABN and DPEN Complexes: PIO Analysis of Phosphine−Pd(II) Interaction and Trans Influence†

Masahiro Yamanaka§ and Koichi Mikami*

Department of Applied Chemistry, Tokyo Institute of Technology, 2-12-1, O-okayama, Meguro-ku, Tokyo, 152-8552, Japan

Received April 4, 2005

The facility of axial chirality control of the Pd(II) complex bearing a chirally flexible (*tropos*) biphenylphosphine (BIPHEP) ligand with combination of diphenylethylenediamine (DPEN) or diaminobinaphthyl (DABN) was theoretically studied by the B3LYP methods and the paired interacting orbital (PIO) analysis. The simple Pd(II) complex models $PR_3Pd(II)$ and $PR_3Pd(II)NMe_3$ (R = H, Ph), were also employed to probe the bonding interaction of the phosphine−Pd(II) moiety and the trans influence of NMe_3 coordination. The PIO analysis of the $PPh_3Pd(II)$ complex indicates that the σ-donation to the vacant Pd 4d orbital is amplified, keeping the π-back-donation to the P−C σ^* orbital by NMe_3 coordination. A similar tendency of the trans influence of the simple model was also observed in the BIPHEP−Pd(II) models. The origin of the strong *atropos* nature of BIPHEP−Pd(II)/DPEN can be caused by enhancement of the σ-interactions with Pd $4d_{xz}$ and $4d_{x^2-y^2}$, which are relatively amplified by coordination of a strongly donative DPEN ligand in comparison with the DABN ligand.

In catalytic asymmetric synthesis, design and development of a chiral ligand have been the key to achieve high enantioselectivity. Metal complexes bearing atropisomeric ligands such as binaphthylphosphine (BINAP) have been widely employed in the asymmetric catalytic reactions.[1] Recently, asymmetric reaction through preferential discrimination of racemic but chirally flexible (*tropos*) catalysts by addition of a certain chemical source has been developed as a new stage of asymmetric catalysis. A racemic metal complex bearing a *tropos* ligand, in principle, can form a single diastereomeric complex with combination of a certain chemical source.[2] In view of the prime importance of the atropisomeric ligand, the enantiopure form of the chirally rigid (*atropos*) BINAP can be replaced by the *tropos* biphenylphosphine (BIPHEP). We have reported that the racemic BIPHEP−Pd(II) complex with the chiral diaminobinaphthyl (DABN) can be used in asymmetric catalysis as an activated diastereomeric complex (Scheme 1).[3]

Scheme 1

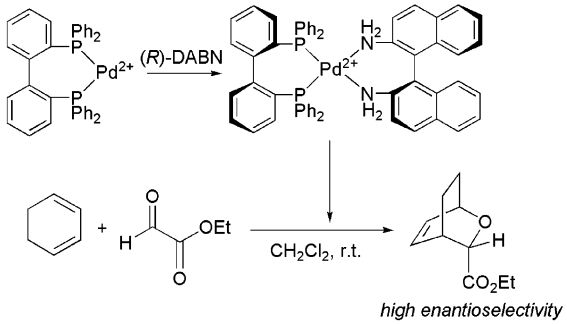

Scheme 2

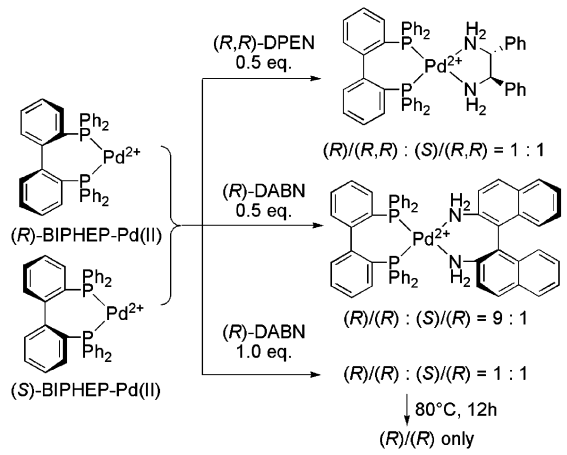

While complexation of racemic BIPHEP−Pd(II) was observed with 1.0 equiv of (*R*)-DABN in a nonselective

† Dedicated to Prof. Iwao Ojima on the occasion of his 60th birthday.

* To whom correspondence should be addressed. E-mail: kmikami@o.cc.titech.ac.jp.

§ Present address: Department of Chemistry, Rikkyo University, 3-34-1, Nishi-Ikebukuro, Toshima-ku, Tokyo, 171-8501, Japan.

(1) (a) Gawley, R. E.; Aube, J. *Principles of Asymmetric Synthesis*; Pergamon: London, 1996. (b) Noyori, R. *Asymmetric Catalysis in Organic Synthesis*; Wiley: New York, 1994. (c) Brunner, H.; Zettlmeier, W. *Handbook of Enantioselective Catalysis*; VCH: Weiheim, 1993. (d) *Catalytic Asymmetric Synthesis*, 2nd ed; Ojima, I. Ed.; VCH: New York, 2000.

(2) (a) Mikami, K.; Matsukawa, S. *Nature* **1997**, *385*, 613−615. (b) Mikami, K.; Matsukawa, S. *Enantiomer* **1996**, *1*, 1−5. (c) Mikami, K.; Terada, M.; Korenaga, T.; Matsumoto, Y.; Ueki, M.; Angelaud, R. *Angew. Chem., Int. Ed.* **2000**, *39*, 3532−3556. (d) Mikami, K.; Terada, M.; Korenaga, T.; Matsukawa, S. *Acc. Chem. Res.* **2000**, *33*, 391. (e) Mikami, K.; Aikawa, K.; Yusa, Y.; Jodry, J. J.; Yamanaka, M. *Synlett* **2002**, 1561.

10.1021/om050249v CCC: $30.25
Publication on Web 08/16/2005

manner, thermodynamically favorable (*R*)-BIPHEP−Pd(II)/(*R*)-DABN was afforded exclusively through *tropo*-inversion of the BIPHEP moiety at 80 °C for 12 h.[3b] Such *atropos* nature of the BIPHEP−Pd(II) moiety was enhanced when chiral diphenylethylenediamine (DPEN) was employed in place of DABN. The 1:1 mixture of BIPHEP−Pd(II)/(*R,R*)-DPEN diastereomers was obtained even from isolated (*R*)-BIPHEP−Pd(II)/(*R,R*)-DPEN after isomerization at 80 °C for 48 h. Complete *tropo*-inversion of the BIPHEP moiety needs a longer time in the DPEN complex than in the DABN complex. The energy difference between two diastereomers is larger in BIPHEP−Pd(II)/DABN than in BIPHEP−Pd(II)/DPEN. The tendency of increasing *atropos* nature by DPEN coordination was also shown in the case of the BIPHEP−Rh(I) complex, where the DABN complex can exhibit *tropo*-inversion at room temperature and the DPEN complex cannot.[4] Our attention is thus directed to facilitate axial chirality control in the BIPHEP−Pd(II)/DABN complex for a long time. To probe this phosphine−Pd interaction issue, two-stage theoretical studies were carried out.

The first stage showed notable characteristics of the phosphine−Pd(II) bonding interaction and trans influence of NMe_3 coordination in simple phosphine−Pd complex models, $PR_3Pd(II)$ and $PR_3Pd(II)NMe_3$ (R = H, Ph). In the second stage, we described theoretical studies on the flexible nature of BIPHEP−Pd(II)/DABN and DPEN in view of the orbital interaction in the phosphine−Pd(II) moiety.

Chemical Models and Computational Methods

The importance of the palladium complex in modern organic synthesis or coordination chemistry is well documented.[5] Although the phosphine−Pd(0) interaction in zerovalent palladium complexes has been reported in detail,[6,7] there is no theoretical study on the phosphine−Pd(II) interaction in cationic divalent palladium complexes. Focusing on the bonding interaction and trans influence in the phosphine−Pd(II) moiety, simple models of Pd(II) complexes, $PR_3Pd(II)$ and $PR_3Pd(II)NMe_3$ (R = H, Ph), were studied first in comparison with $PH_3Pd(0)$. The BIPHEP−Pd(II)/DABN and DPEN complexes regarded as the real models were next compared to examine the reason why chirality control on BIPHEP−Pd(II)/DABN is easier than on BIPHEP−Pd(II)/DPEN.

Geometry optimizations, energetics, and canonical molecular orbital (MO) analysis of the simple and realistic models were carried out by B3LYP[8] and ONIOM(B3LYP:HF)[9] calculations, respectively. All calculations were performed with the Gaussian 98 package.[10] The simple models, $PR_3Pd(II)$ and $PR_3Pd(II)NMe_3$, were optimized by the B3LYP method with the basis set denoted as 631SDD consisting of the Sttutgart effective core potential (SDD)[11] for Pd and the 6-31G(d) basis set[12] for the rest. The real models, BIPHEP−Pd(II)/DABN and DPEN, were calculated using the ONIOM methods, which have been proven to be a powerful tool for the theoretical treatment of large molecular systems. We divided the real system of the BIPHEP−Pd(II)/DABN and DPEN complexes into two layers as shown in Figure 1.[13] The small models of layer-1 were treated at the B3LYP/631SDD level, and the fully real models of layer-2 were treated by the HF method with the basis set denoted as 321LAN consisting of the LANL2DZ effective core potential[14] for Pd and the 3-21G basis set for the rest.[12]

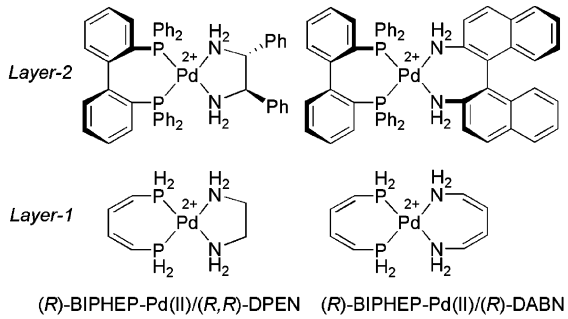

Figure 1. Chemical models of BIPHEP−Pd(II)/DPEN and DABN.

In the realistic BIPHEP−Pd(II) complexes having a large number of MOs, not only the frontier MOs but also the relevant MOs should participate significantly in orbital interactions in the phosphine−Pd(II) region. However, it is difficult to identify such interacting orbitals due to delocalization of the canonical MOs in the large Pd complexes such as BIPHEP−Pd(II). We thus carried out paired interacting orbital (PIO) analysis[15] on the orbital interaction analysis software "LUMMOX"[6d,16,17] to illustrate the primary orbital interaction

(3) (a) Mikami, K.; Aikawa, K.; Yusa, Y.; Hatano, M. *Org. Lett.* **2002**, *4*, 91−94 (b) Mikami, K.; Aikawa, K.; Yusa, Y. *Org. Lett.* **2002**, *4*, 95−98.

(4) Mikami, K.; Kataoka, S.; Yusa, Y.; Aikawa, K. *Org. Lett.* **2004**, *6*, 3699−3701.

(5) (a) Collman, J. P.; Hegedus, L. S.; Norton, J. R.; Finke, R. G. *Principals and Applications of Organotransition Metal Chemistry*; University Science Books: Mill Valley, CA, 1987. (b) Cotton, F. A.; Wilkinson, G. *Advanced Inorganic Chemistry*, 5th ed.; Wiley-Interscience: New York, 1988.

(6) (a) Xiao, S.-X.; Trogler, W. C.; Ellis, D. E.; Berkovitch-Yellin, Z. *J. Am. Chem. Soc.* **1983**, *105*, 7033−7037. (b) Marynick, D. S. *J. Am. Chem. Soc.* **1984**, *106*, 4065−4066. (c) Pacchioni, G.; Bagus, P. S. *Inorg. Chem.* **1992**, *31*, 4391−4398. (d) Yamanaka, M.; Shiga, A. *J. Theor. Comput. Chem.* **2005**, *4*, 345−355.

(7) (a) Orpen, A. G.; Connelly, N. G. *J. Chem. Soc., Chem. Commun.* **1985**, 1310−1311. (b) Tossell, J. A.; Moore, J. H.; Giordan, J. C. *Inorg. Chem.* 1985, *24*, 1100−1103. (c) Orpen, A. G.; Connelly, N. G. *Organometallics* **1990**, *9*, 1206−1210.

(8) (a) Becke, A. D. *J. Chem. Phys.* **1993**, *98*, 5648−5652. (b) Lee, C.; Yang, W.; Parr, R. G. *Phys. Rev. B* **1988**, *37*, 785−789.

(9) (a) Maseras, F.; Morokuma, K. *J. Comput. Chem.* **1995**, *16*, 1170−1179. (b) Svensson, M.; Humbel, S.; Froese, R. D. J.; Matsubara, T.; Sieber, S.; Morokuma, K. *J. Phys. Chem.* **1996**, *100*, 19357−19363. (c) Dapprich, S.; Komaromi, I.; Byun, K. S.; Morokuma, K.; Frisch, M. J. *J. Mol. Struct. (THEOCHEM)* **1999**, *461−462*, 1−21. (d) Vreven, T.; Morokuma, K. *J. Comput. Chem.* **2000**, *21*, 1419−1432.

(10) Frisch, M. J.; Trucks, G. W.; Schlegel, H. B.; Scuseria, G. E.; Robb, M. A.; Cheeseman, J. R.; Zakrzewski, V. G.; Montgomery, J. A., Jr.; Stratmann, R. E.; Burant, J. C.; Dapprich, S.; Millam, J. M.; Daniels, A. D.; Kudin, K. N.; Strain, M. C.; Farkas, O.; Tomasi, J.; Barone, V.; Cossi, M.; Cammi, R.; Mennucci, B.; Pomelli, C.; Adamo, C.; Clifford, S.; Ochterski, J.; Petersson, G. A.; Ayala, P. Y.; Cui, Q.; Morokuma, K.; Salvador, P.; Dannenberg, J. J.; Malick, D. K.; Rabuck, A. D.; Raghavachari, K.; Foresman, J. B.; Cioslowski, J.; Ortiz, J. V.; Baboul, A. G.; Stefanov, B. B.; Liu, G.; Liashenko, A.; Piskorz, P.; Komaromi, I.; Gomperts, R.; Martin, R. L.; Fox, D. J.; Keith, T.; Al-Laham, M. A.; Peng, C. Y.; Nanayakkara, A.; Challacombe, M.; Gill, P. M. W.; Johnson, B.; Chen, W.; Wong, M. W.; Andres, J. L.; Gonzalez, C.; Head-Gordon, M.; Replogle, E. S.; Pople, J. A. *Gaussian 98*, Revision A.11; Gaussian, Inc.: Pittsburgh, PA, 2001.

(11) Dolg, M.; Wedig, U.; Stoll, H.; Preuss, H. *J. Chem. Phys.* **1987**, *86*, 866−872.

(12) Hehre, W. J.; Radom, L.; Schleyer, P. v. R.; Pople, J. A. *Ab initio Molecular Orbital Theory*; John Wiley: New York, 1986, and references cited therein.

(13) Yamanaka, M.; Mikami, K. *Organometallics* **2002**, *21*, 5847−5851.

(14) Wadt, W. R.; Hay, P. J. *J. Chem. Phys.* **1985**, *82*, 299−310.

(15) (a) Fujimoto, H. *Acc. Chem. Res.* **1987**, *20*, 448. (b) Fujimoto, H.; Mizutani, Y.; Endo, J.; Jinbu, Y. *J. Org. Chem.* **1989**, *54*, 2568. (c) Suzuki, T.; Okada, G.; Hioki, Y.; Fujimoto, H. *Organometallics* **2003**, *22*, 3649.

(16) Katsumi, H.; Kikuzono, Y.; Yoshida, M.; Shiga, A.; Fujimoto, H. *LUMMOX* ver.1.1; Sumitomochemical Co. Ltd.: Tokyo, 1999. LUMMOX is built up using Visual Basic 6.0 and Visual C++ 6.0, and runs on Windows PC with Windows95 and higher.

(17) (a) Shiga, A. *Res. Chem. Intermed.* **2002**, *28*, 485. (b) Hosokawa, T.; Nakano, K.; Kobiro, K.; Shiga, A. *Tetrahedron Lett.* **2003**, *44*, 1175. (c) Takao M.; Shiga, A. *J. Comput. Chem.* **2004**, *25*, 106, and references therein.

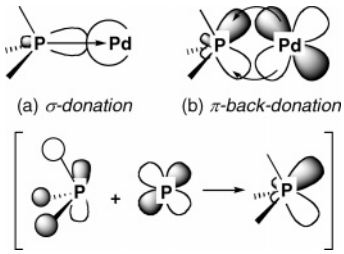

Figure 2. Schematic representation of conventional phosphine−Pd bonding interactions of (a) σ-donation and (b) π-back-donation.

in the phosphine−Pd(II) complexes. The novel concept of PIO was developed by Fujimoto to make it possible to find pairs of relevant MOs for various types of chemical interactions between two fragments (e.g., phosphine ligand and palladium atom) in the interacting composite system (e.g., phosphine−palladium complex). The basic idea of the PIO analysis stems from the hybrid orbital concept: a carbon−carbon single bond can be visualized more concisely by a combination of two sp^3 hybrid atomic orbitals of those carbons rather than a combination of atomic orbitals. The PIO analysis on LUMMOX of the optimized structures by the B3LYP or ONIOM(B3LYP:HF) method was carried out using the extended Hückel method based on the Wolfsberg−Helmholtz method.[18]

PR_3Pd and PR_3PdNMe_3 Studies

It has been widely and conventionally accepted that the orbital interaction in the phosphine−Pd bonding consists of σ-donating and π-accepting components (Figure 2).[19] The P lone pair of the PR_3 ligand donates to the empty orbital on the Pd, and the filled Pd d orbitals back-donate to the empty P−R σ^* orbitals. Aspects of the π-back-donation, in particular, have been discussed by ab initio calculations[6] and the experimental metal−phosphine and P−R bond lengths.[7] In the phosphine LUMOs, the σ^* orbitals mix into the empty 3d orbitals to form well-hybridized π-accepting orbitals (Figure 2b). The issue of σ-basicity and π-acidity of phosphine ligands in PR_3Pd complexes has been predicted by ab initio calculations only for the free PR_3.[6a,20] These theoretical and experimental evidences were limited to neutral zerovalent palladium complexes or other transition-metal complexes instead of the importance of cationic divalent palladium species in synthetic and coordination chemistry. Therefore, we first studied the substituent effect in PR_3 ligands and the trans influence of NMe_3 coordination on the $PR_3Pd(II)$ complexes from the interacting orbital viewpoint.

The simple models of Pd complexes, PR_3Pd and PR_3PdNMe_3 (R = H, Ph), were studied at the B3LYP/631SDD level (Table 1). The longer P−H length (r1) in $PH_3Pd(0)$ than that in $PH_3Pd(II)$ indicates that π-back-donation largely contributes to the bonding interaction in $PH_3Pd(0)$. The phosphine−Pd interaction energies (ΔE) were much larger in $PH_3Pd(II)$ than in $PH_3Pd(0)$. This indicates that the electrostatic interaction is more affected in the Pd(II) complexes than in the Pd(0) complexes. The ΔE values become much smaller in the Pd(II) complexes and larger in the Pd(0) complexes by coordination of NMe_3 trans to PR_3. In $PH_3Pd(0)$, no

Table 1. Details of the Geometries in PR_3Pd (1) and PR_3PdNMe_3 (2) Models Optimized by B3LYP/631SDD

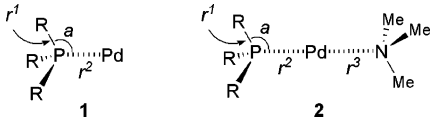

1 **2**

	Pd	PR_3	r^1 (Å)	r^2 (Å)	r^3 (Å)	a	ΔE (kcal/mol)
1a	Pd(II)	PH_3	1.414	2.313		106.3°	−230.0
1b	Pd(II)	PPh_3	1.780	2.234		99.9°	−385.4
1c	Pd(0)	PH_3	1.420	2.209		121.1°	−34.5
2a	Pd(II)	PH_3	1.406	2.420	2.067	114.6°	−72.4
2b	Pd(II)	PPh_3	1.792	2.263	2.205	103.4°	−175.2
2c	Pd(0)	PH_3	1.423	2.209	2.242	121.5°	−38.9

drastic structural change was found by coordination of NMe_3. In sharp contrast, the PH_3−Pd(II) distance, in particular, was lengthened by ca. 0.11 Å. The distance of PPh_3−Pd(II) did not change drastically even by coordination of NMe_3. These differences of structural properties between Pd(0) and Pd(II) complexes should be caused mainly by the difference of the orbital interaction.

To explain the difference between Pd(0) and Pd(II) complexes, Kohn−Sham orbitals (KOs) of $PH_3Pd(0)$, $PH_3Pd(II)$, and $PPh_3Pd(II)$ were studied in detail. It is noted that the four-electron interaction, namely, the Occ−Occ orbital interaction, between the P−R σ orbital and the Pd d orbital was observed in both Pd(0) and Pd(II) complexes (Figures 3 and 4). The $PH_3Pd(0)$ complex, in particular, showed simultaneously the orbital interaction between the P−H σ^* orbital and the Pd(0) d orbital (Figure 3a). The four-electron interaction in the presence of a third higher lying empty orbital can generally stabilize the interacting system.[21] In the $PH_3Pd(0)$ complex, therefore, the Occ−Occ orbital interaction between the Pd(0) d orbital and the P−R σ orbital should elevate the energy level of the hybridized Pd(0) d orbital to interact readily with the P−R σ^* orbital (KO12, KO15, and KO24 in Figure 3). In turn, the P−H σ orbital mixes into the P−H σ^* orbital through interaction with the Pd(0) d orbital. The Occ−Occ orbital interaction between the Pd(0) d orbital and the P−H σ orbital results in strengthening the π-back-donation in $PH_3Pd(0)$. Thus, the conventional Occ−Unocc interacting π-back-donation in the phosphine−Pd(0) complex could be revised to the three molecular orbital, four-electron model as shown in Figure 3e.[6d]

On the other hand, such a three molecular orbital, four-electron interaction between PR_3 ligands and Pd cannot be found in either $PH_3Pd(II)$ or $PPh_3Pd(II)$. While the Occ−Occ orbital interaction between the P−R σ orbital and the Pd(II) d orbital was observed, there is no π-back-donative interaction to the P−R σ^* orbital (Figure 4). The lower lying d orbital of the cationic Pd(II) center rarely interacts with the P−R σ^* orbital even when the Occ−Occ interaction forms the hybridized Pd(II) d orbital. In sharp contrast to $PH_3Pd(0)$, the phosphine−Pd(II) complexes mainly consist of the σ-donative interaction between the p orbital of P and the vacant 4d orbital of Pd(II) (Figures 4b and f).

(18) Wolfsberg, M.; Helmholtz, L. *J. Chem. Phys.* **1952**, *26*, 837.
(19) (a) Dewar, M. J. S. *Bull. Soc. Chem. Fr.* **1951**, *C71*, 18. (b) Chatt, J.; Duncanson, L. A. *J. Chem. Soc.* **1953**, 2939.
(20) Pacchioni, G.; Bagus, P. S. *Inorg. Chem.* **1992**, *31*, 4391.
(21) (a) Inagaki, S.; Fujimoto, H.; Fukui, K. *J. Am. Chem. Soc.* **1976**, *98*, 4054. (b) Bach, R. D.; Wolber, G. J. *J. Am. Chem. Soc.* **1984**, *106*, 1401. (c) Bach, R. D.; Wolber, G. J. *J. Am. Chem. Soc.* **1984**, *106*, 1410.

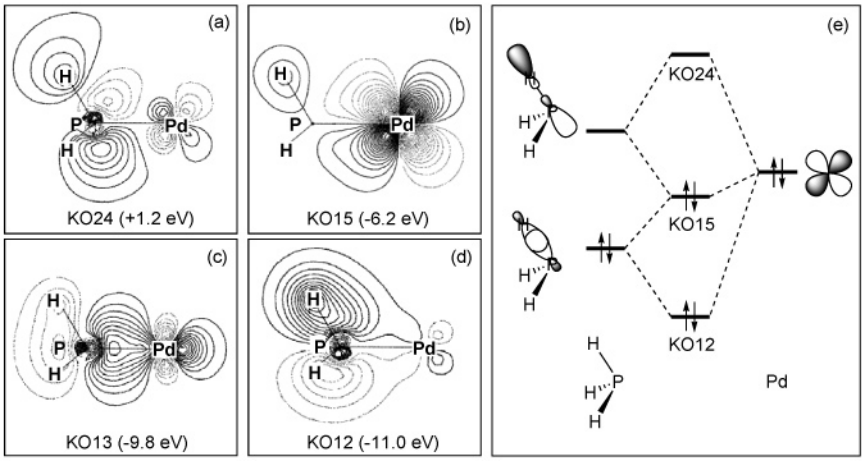

Figure 3. Kohn−Sham orbitals of (a, b, d) π-back-donation and (c) σ-donation, and (e) schematic three molecular orbital, four-electron model of the π-back-donation in $PH_3Pd(0)$.

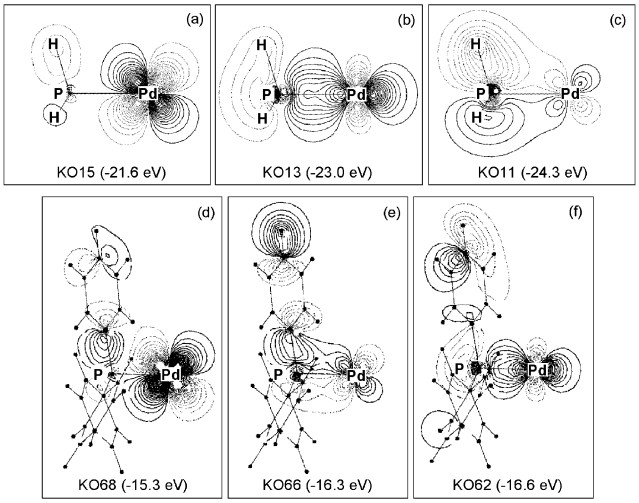

Figure 4. Kohn−Sham orbitals of π- and σ-components of the bonding interaction in (a, b, c) $PH_3Pd(II)$ and (d, e, f) $PPh_3Pd(II)$.

Next, PIO analysis based on the extended Hückel method was employed for the PR_3Pd and PR_3PdNMe_3 complexes optimized at the B3LYP/631SDD level. The orbital interaction analysis system "LUMMOX" clearly shows that the contribution of σ-donation and π-back-donation to the bonding interaction in the Pd(0) complex dramatically changes in the Pd(II) complex. The PR_3Pd models were divided into the Pd and PR_3 fragments (R = H, Ph). The major PIOs participating dominantly in the orbital interaction between Pd and PR_3 were regarded as the σ- and π-components (Figure 5). The large overlap population (OP) indicates the strong orbital interaction between Pd and PR_3 fragments. The occupation number (ON) shows the number of electrons in the interacting orbital pair, and hence the ideal Occ−Unocc orbital interaction should involve an ON of just 2.0. The mixing into the lower lying occupied orbital could occur when the ON exceeds 2.0. In both the Pd(0) and Pd(II) complexes, the much larger OP of the σ-donation than that of the π-back-donation indicates that the primary PIOs are σ-donation (Figure 5). In sharp contrast to the σ-donation, where the ON is ca. 2.0 due to the typical Occ−Unocc interaction, an ON of the π-back-donation in excess of 2.0 should be caused by a three molecular orbital, four-electron interaction (Figure 3e). The bonding interaction in $PH_3Pd(0)$ mainly consists of the σ-donation (PIO-1), but π-back-donation (PIOs-2,3) participates in the bonding interaction. The σ-donation is caused by the interaction between the p orbital on P and the vacant 5s orbital on Pd(0). As shown in the KOs of $PH_3Pd(0)$, the Occ−Occ interaction between the Pd(0) d orbital and the P−H σ orbital is applied in the PIOs-2,3 because the ON exceeds 2.0. On the other hand, the σ-donation consisting of the p orbital on P and the vacant 4d orbital on Pd(II) remarkably participates in the bonding interaction in the Pd(II) complexes due to smaller OP values of the π-back-donation (PIOs-2,3 in $PH_3Pd(II)$, PIOs-3,4 in $PPh_3Pd(II)$). The PIO-2 in PPh_3-Pd(II) showed another type of σ-donation, which is derived from the interaction between the p orbital on P and the vacant 5s orbital on Pd(II). The ON relatively increases in the π-back-donation of both $PH_3Pd(II)$ and $PPh_3Pd(II)$ in comparison with $PH_3Pd(0)$. These results of smaller OP and larger ON observed in the π-back-donation on $PH_3Pd(II)$ and $PPh_3Pd(II)$ are comparable to KOs, where no π-back-donation was found.

The trans influence of NMe_3 ligand, which is one of the fundamental topics in the coordination chemistry, was observed in the PH_3Pd and PPh_3Pd complexes (Figures 6 and 7). The PR_3PdNMe_3 models were first divided into $PdNMe_3$ and PR_3 fragments (R = H, Ph). The primary PIOs of the bonding interaction between PR_3 and Pd dramatically change from donative to a back-donative interaction in the NMe_3-coordinating Pd(0) complex (Figure 6a). Coordination of NMe_3 on Pd(0) trans to PH_3 enhanced considerably the π-back-donation in $PH_3Pd(0)NMe_3$ due to an increase of OP and a decrease of ON in PIOs-1,2. A similar but slight trend was observed in $PH_3Pd(II)NMe_3$ (Figures 6b). In $PPh_3Pd(II)NMe_3$, NMe coordination emphasizes the σ-donation (PIO-1) as well as the π-back-donation (PIOs-3,4) (Figure 6c). To clarify the role of NMe_3 coordination in the enhancement of π-back-donation on PR_3PdNMe_3, the PIOs were also examined by dividing PR_3PdNMe_3 into PR_3Pd and NMe_3 fragments (Figure 7). Three pairs of interacting orbitals participate dominantly in the bonding interaction in $PR_3Pd-NMe_3$, involving σ- and π-components. The π-component having the negative OP (i.e., out-of-phase interaction) and the large ON (over 3.0) indicates that the Pd d orbital interacts with the N−C σ orbital. Therefore, increase of the π-back-

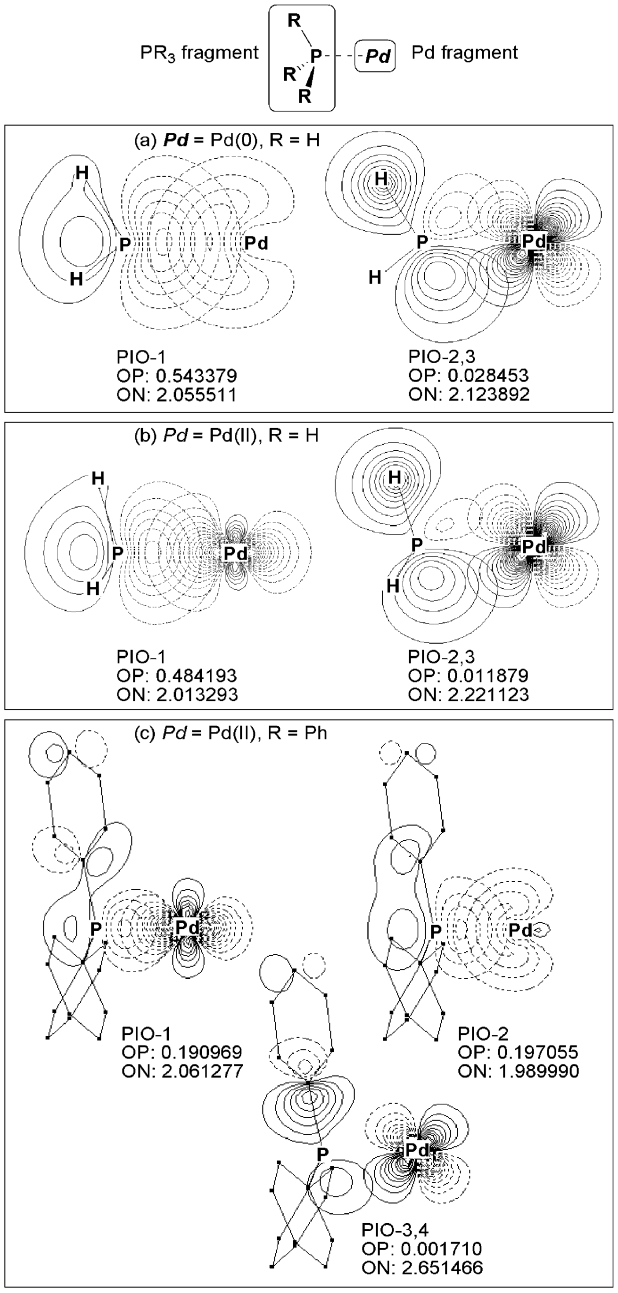

Figure 5. Major PIOs of (a) $PH_3Pd(II)$, (b) $PH_3Pd(II)$, and (c) $PPh_3Pd(II)$. OP: overlap population. ON: occupation number.

donation by NMe_3 coordination is caused by raising the energy level of the Pd d orbital due to the Occ−Occ orbital interaction between the Pd d orbital and the N−C σ orbital. The PIO analysis supported a similar role of NMe_3 coordination to mixing the P−H σ orbital, which elevates the energy level of the Pd d orbital to emphasize the π-back-donation. On the other hand, NMe_3 coordination weakened the σ-donation in $PH_3Pd(0)$ and $PH_3Pd(II)$, where a relatively smaller OP was observed by NMe_3 coordination (Figures 6a and b). In sharp contrast, a notable increase in OP of PIO-1 and a slight decrease in OP of PIO-2 were shown in the σ-component of the bonding interaction in $PPh_3Pd(II)$-NMe_3 (Figure 6c). The higher lying lone-pair p orbital of PPh_3 readily interacts with the vacant d orbital of Pd(II) elevated energetically by interaction with the lone-pair p orbital of NMe_3. In the case of $PH_3Pd(II)$-

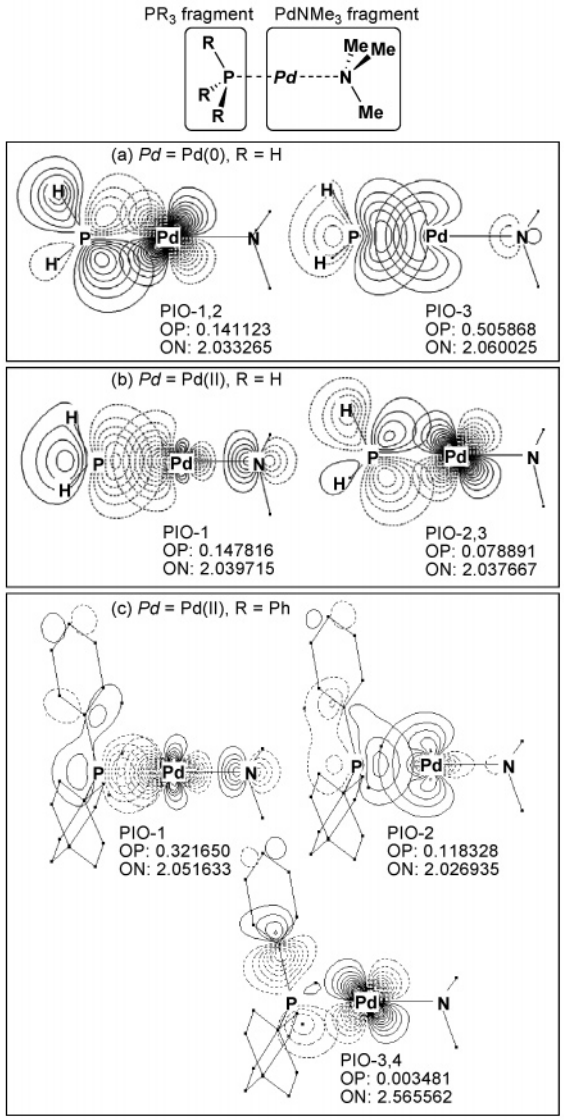

Figure 6. Major PIOs of (a) $PH_3Pd(0)NMe_3$, (b) PH_3-$Pd(II)NMe_3$, and (c) $PPh_3Pd(II)NMe_3$ by dividing into PR_3 and $PdNMe_3$ fragments. OP: overlap population. ON: occupation number.

NMe_3, this interaction of NMe_3 with Pd(II) increases the energy gap (i.e., weakens the interaction) between the lower lying lone-pair p orbital of PH_3 and the vacant d orbital of Pd(II). The substituent effect in PR_3 ligands and the trans influence of NMe_3 coordination on PH_3-Pd(II) and $PPh_3Pd(II)$ were studied. It was illustrated that the σ-component in the bonding interaction dominantly participates in the Pd(II) complexes in comparison with $PH_3Pd(0)$. NMe_3 coordination shows remarkably the substituted effect of the PR_3 ligand; the π-back-donation in the case of PH_3 and σ-donation in the case of PPh_3 are enhanced by coordination of NMe_3, respectively.

BIPHEP−Pd(II), BIPHEP−Pd(II)/DPEN, and BIPHEP−Pd(II)/DABN Studies

The flexibile nature of the BIPHEP−Pd(II)/DPEN and DABN complexes was theoretically studied based on the bonding interaction in the phosphine−Pd(II) moiety as shown in the previous section. Two diastereomers of the BIPHEP−Pd(II)/DPEN and DABN com-

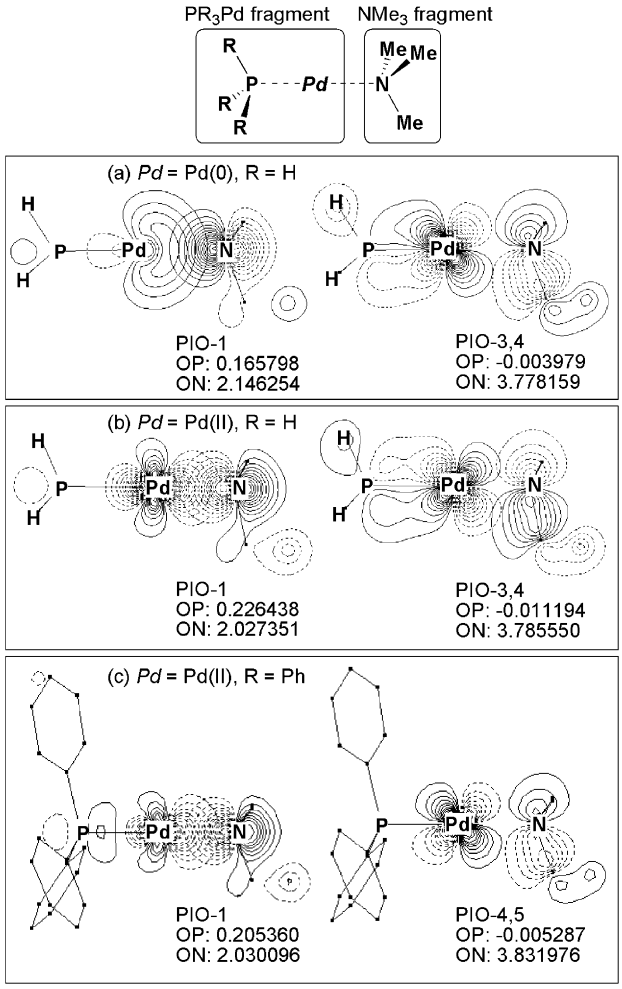

Figure 7. Major PIOs of (a) $PH_3Pd(0)NMe_3$, (b) $PH_3Pd(II)NMe_3$, and (c) $PPh_3Pd(II)NMe_3$ by dividing into PR_3Pd and NMe_3 fragments. OP: overlap population. ON: occupation number.

plexes were optimized by the ONIOM(B3LYP:HF) calculation (Figure 8 and Table 2). The relative energies of BIPHEP−Pd(II)/DPEN and DABN complexes were obtained at the B3LYP/631SDD//ONIOM(B3LYP/631SDD:HF/321LAN) level. In agreement with experimental results as described above, the energy difference between favorable (*R*)-**3** and unfavorable (*S*)-**3** complexes was only 0.3 kcal/mol in BIPHEP−Pd(II)/DPEN (a series) and 5.8 kcal/mol in BIPHEP−Pd(II)/DABN (b series). As shown in Table 2, almost the same structure around the Pd(II) center was found in both diastereomers, (*R*)-**3a** and (*S*)-**3a**, of BIPHEP−Pd(II)/DPEN. On the other hand, BIPHEP−Pd(II)/DABN has obvious differences in the structural properties around the Pd(II) center between the (*R*)-**3b** and (*S*)-**3b** diastereomers. The larger structural differences between the two diastereomers observed in BIPHEP−Pd(II)/DABN could be caused by the steric repulsion between the phenyl group of BIPHEP and the naphthyl group of DABN (Figure 8).

To probe the bonding interaction between BIPHEP and Pd(II), KOs of BIPHEP−Pd(II) were studied in detail (Figure 9). There are numerous KOs consisting of the p orbitals on the carbon atoms of the aromatic rings (gray line in Figure 9), while the Pd(II) d orbitals were identified below the energy level of the frontier region (bold line in Figure 9). It is found that KO146

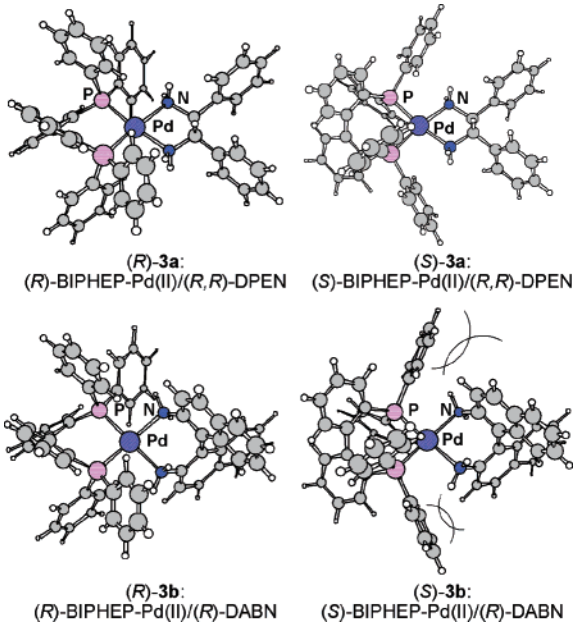

Figure 8. 3D structures of the two diastereomers in BIPHEP−Pd(II)/DPEN (**3a**) and BIPHEP−Pd(II)/DABN (**3b**) optimized by ONIOM(B3LYP/631SDD:HF/321LAN).

Table 2. Details of the Geometries the Two Diastereomers in BIPHEP−Pd(II)/DPEN (3a) and BIPHEP−Pd(II)/DABN (3b) Optimized by ONIOM(B3LYP/631SDD:HF/321LAN)

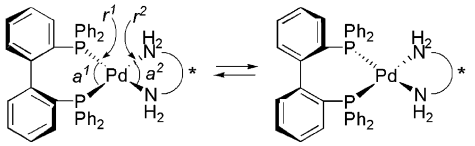

	Diamine	r^1 (A)	r^2 (A)	a^1 (deg.)	a^2 (deg.)	ΔE (kcal/mol)[a]
(*R*)-**3a**		2.318	2.163	93.1	78.8	0.0
(*S*)-**3a**		2.310	2.169	93.6	78.7	+0.3
(*R*)-**3b**		2.310	2.234	92.7	85.7	0.0
(*S*)-**3b**		2.340	2.228	91.8	83.5	+5.8

[a] Single-point energy calculations at the B3LYP/631SDD level using geometries optimized by ONIOM(B3YLP/631SDD;HF/321LAN).

(the lowest unoccupied orbital) and KO111 are derived from the in-phase and the out-of-phase interactions between the Pd(II) d_{xy} orbital and the lone-pair p orbital of BIPHEP. A notably large energy gap (ca. 7 eV) between KO146 and KO111 indicates that the bonding interaction of the Pd(II) d_{xy} orbital with the lone-pair orbital of BIPHEP is much stronger. The Occ−Occ interactions between the P−C σ orbitals and the Pd(II) d orbitals were observed (partially localized on Pd: KO131 and KO132; partially localized on BIPHEP: KO126 and KO128). No π-back-donative interaction described as a three molecular orbital, four-electron model, however, was found in BIPHEP−Pd(II). In a similar manner to the PPh_3−Pd(II) bonding interaction, the BIPHEP−Pd(II) bonding interaction is constructed mainly by σ-donation. Unfortunately, the large number

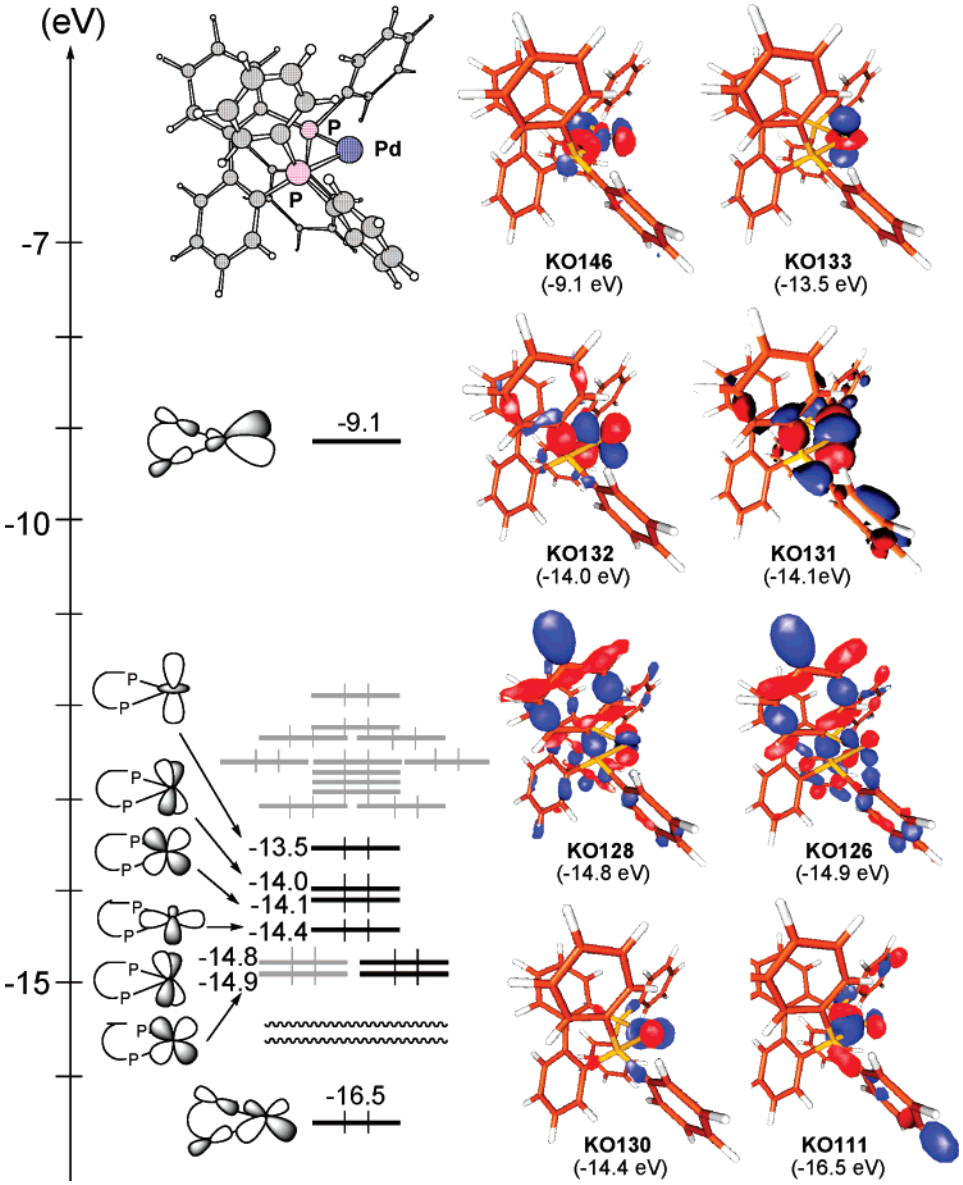

Figure 9. Kohn−Sham orbitals containing Pd(II) d orbitals of BIPHEP−Pd(II).

Table 3. Values of Overlap Population (OP) and Occupation Number (ON) in PIOs of (*R*)-BIPHEP−Pd(II), (*R*)-BIPHEP−Pd(II)/(*R*,*R*)-DPEN, and (*R*)-BIPHEP−Pd(II)/(*R*)-DABN

	PIO-1	PIO-2	PIO-3	PIO-4	PIO-5
(*R*)-BIPHEP−Pd(II)	OP: 0.276005	OP: 0.417068	OP: 0.003847	OP: 0.008974	OP: 0.004188
	ON: 2.062709	ON: 2.063653	ON: 2.572537	ON: 2.561332	ON: 2.373629
(*R*)-BIHEP−Pd(II)/(*R*,*R*)-DPEN	OP: 0.419947	OP: 0.382611	OP: 0.080338	OP: 0.010206	OP: 0.009101
	ON: 2.038228	ON: 2.215493	ON: 2.340875	ON: 2.310270	ON: 2.425108
(*R*)-BIHEP−Pd(II)/(*R*)-DABN	OP: 0.405912	OP: 0.389839	OP: 0.64938	OP: 0.010800	OP: 0.009262
	ON: 2.038989	ON: 2.203163	ON: 2.433822	ON: 2.408174	ON: 2.452932

of KOs in BIPHEP−Pd(II)/DPEN and DABN are too complicated to study on the flexible nature of the BIPHEP moiety.

Next, PIO analysis based on the extend Hückel method was employed for (*R*)-BIPHEP−Pd(II), (*R*)-BIPHEP−Pd(II)/(*R*,*R*)-DPEN, and (*R*)-BIPHEP−Pd(II)/(*R*)-DABN optimized by the ONIOM(B3LYP:HF) method (Figures 10, 11, and 12). The data of OP and ON of the five major PIOs observed in each complexes are summarized in Table 3. As shown in Figure 10, the five major PIOs in BIPHEP−Pd(II) were identified as $4d_{xy}$ (PIO-1), 5s (PIO-2), $4d_{x^2-y^2}$ (PIO-3), $4d_{yz}$ (PIO-4), and $4d_{xz}$ (PIO-5), respectively (Pd $4d_{z^2}$ orbital found in the minor PIO). The PIOs-1 and -2 having relatively large OP (Table 3) indicate that BIPHEP−Pd(II) mainly consists of σ-donation, as shown in KO study (KOs 146 and 111 in Figure 9). The PIOs-1 and -2 have an ON of just 2.0 due to the ideal Occ−Unocc orbital interaction (vacant $4d_{xy}$ in PIO-1 and 5s in PIO-2). The PIOs-4 and -5 corresponding to the Occ−Occ interaction between the P−C σ orbital and the Pd(II) d orbital (KOs 126, 128, 131, and 132 in Figure 9) show small values of OP and ONs of more than 2.0.

The five major PIOs in BIPHEP−Pd(II)/DPEN and DABN are almost the same as in BIPHEP−Pd(II), while PIO-4 and PIO-5 are switched with each other by

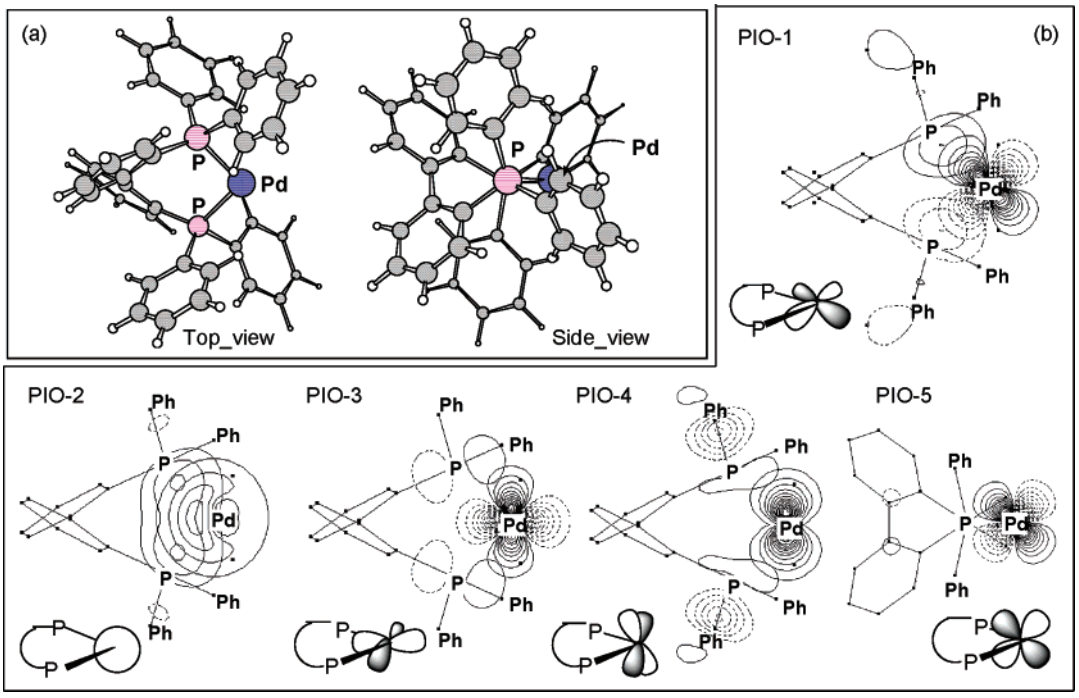

Figure 10. (a) 3D structure and (b) the five major PIOs of (*R*)-BIPHEP−Pd(II). OP: overlap population. ON: occupation number.

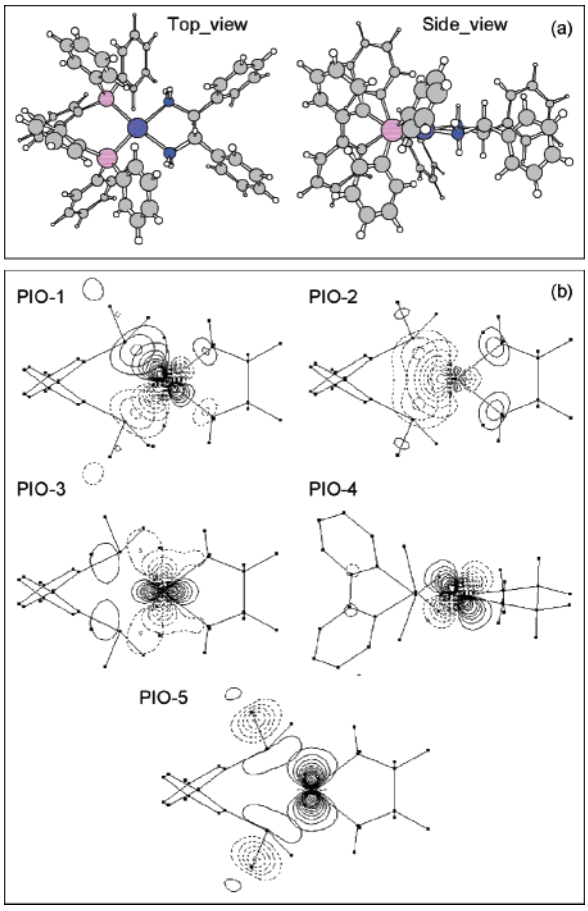

Figure 11. (a) 3D structure and (b) the five major PIOs of (*R*)-BIPHEP−Pd(II)/(*R,R*)-DPEN. OP: overlap population. ON: occupation number.

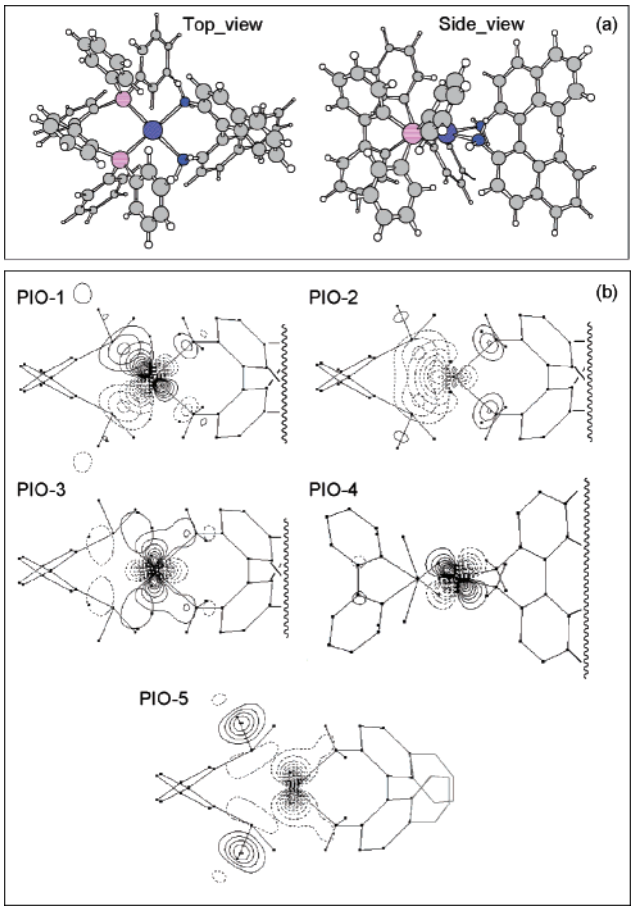

Figure 12. (a) 3D structure and (b) the five major PIOs of (*R*)-BIPHEP−Pd(II)/(*R*)-DABN. OP: overlap population. ON: occupation number.

complexation of DPEN or DABN (Figures 11 and 12). In both BIPHEP−Pd(II)/DPEN and DABN, it is noted that the OP of the PIOs-1 and -3 consisting of a σ-component remarkably increases, while the ON slightly decreases. The PIO-2 of the σ-donation between the p orbital on P and the vacant Pd(II) 5s orbital showed a

slight decrease in the OP. On the other hand, the PIOs-4 and -5 consisting of a π-component showed almost the same OP and a decrease of ON. These effects by complexation of DPEN or DABN are similar to those observed in the trans influence of $PPh_3Pd(II)NMe_3$. Compared with the difference in the OP between BIPHEP−Pd(II)/DPEN and DABN, the PIOs-1 and -3 show larger OPs in the DPEN complex than in the DABN complex (Table 3). Almost the same OP was obtained in other PIOs of both the DPEN and the DABN complexes. Therefore, the *atropos* nature in BIPHEP−Pd(II)/DPEN is caused by the stronger bonding interaction of the σ-donation shown in PIOs-1 and -3 (Figures 11 and 12).

In conclusion, the bonding interaction of σ-interactions with Pd $4d_{xzy}$ and $4d_{x^2-y^2}$ in $PPh_3Pd(II)$ and BIPEHP−Pd(II) is relatively amplified by coordination of strongly donative amine ligand such as DPEN. The present basic theory on the bonding interaction of the phosphine−Pd(II) complex can be applied to the design and development of phosphine ligands, in particular, chirally flexible ligands, which provide a general and powerful strategy for asymmetric catalysis without enantiomeric resolution.

OM050249V